Electronic supplementary materials *Mendeleev Commun.*, 2022, **32**, 531–533

Photo- and ionochromic properties of new spirobenzochromene-pyranoquinoline

Anatoly V. Chernyshev, Ekaterina V. Solov'eva, Irina A. Rostovtseva, Nikolai A. Voloshin, Oleg P. Demidov, Konstantin E. Shepelenko and Anatoly V. Metelitsa

Experimental part

A. Materials and methods

The electronic absorption spectra have been recorded on an "Agilent 8453" spectrophotometer equipped with a temperature-controlled cell. Fluorescence emission and excitation spectra were collected using an Eclipse Varian spectrofluorimeter. Irradiation light was brought into the thermostated cell compartment at 90° from a 200 W high-pressure mercury lamp "Newport" equipped with glass filters for the allocation of mercury lines.

NMR spectra were recorded on a Bruker Avance Neo 300 (300 MHz, ^{1}H, 75 MHz,^{13}C) spectrometer. Chemical shifts are referenced to the residual ^{1}H peak at 7.24 ppm or ^{13}C peak at 77.16 ppm in $CDCl_3$. Data were reported as follows: chemical shift, multiplicity, coupling constant (*J*), integration, and proton signal assignments. Multiplicities are reported as singlet (s), doublet (d), doublet of doublets (dd), doublet of a doublet of doublets (ddd), multiplet (m). Chemical shift values are reported in ppm. All coupling constants (*J*) are reported in Hertz (Hz). The proton NMR signal assignments were performed using COSY 2D NMR technique. The carbon NMR signal assignments were performed employing HSQC and HMBC 2D NMR techniques. High-resolution mass spectra were obtained from a TOF mass spectrometer with an ESI source (BrukermaXis). The instrument was operated in positive mode using an m/z range of 50–3000. The capillary voltage of the ion source was set at 4500 V. The nebulizer gas pressure was 0.4bar, the drying gas flow was set to 4.0 $L \cdot min^{-1}$. Elemental analysis was carried out using a KOVO CHN analyzer. Melting points were measured on a Boetius microscopic hotstage and are uncorrected. The reagents and solvents were all purchased from commercial suppliers and used without further purification. To prepare solutions for spectrophotometry and fluorescence study acetone of the spectroscopic grade has been used. All the metal salts were perchlorates.

The X-ray diffraction data set was recorded on an Agilent SuperNova diffractometer using a microfocus X-ray radiation source with the copper anode (Cu Kα (λ = 1.54184)) and Atlas S2 two-dimensional CCD detector. The reflections were recorded and unit cell parameters were determined and refined using the dedicated CrysAlisPro 171.41.93a software suite [S1]. The

structure was solved with ShelXT program [S2] and refined with ShelXL program [S3], the graphics were rendered using the Olex2 ver 1.3.0 software suite [S4]. The complete X-ray structural dataset for compound **1** was deposited at the Cambridge Crystallographic Data Center (deposit CCDC 2123459). Crystals suitable for X-ray structural analysis were obtained by slow evaporation of toluene at room temperature. *Crystal data for* **1**. A light yellow crystal, $C_{25}H_{16}ClNO_2$, (M = 397.84), orthorhombic, space group *Pbca* (no. 61), a = 11.5038(3) Å, b = 6.5637(2) Å, c = 49.8431(14) Å, V = 3763.53(18) Å^3, Z = 8, T = 100.00(10) K, μ(Cu Kα) = 1.972 mm^{-1}, d_{calc} = 1.404 g cm^{-3}, 20085 reflections measured (7.094° ≤ 2θ ≤ 154.032°), 3945 unique (R_{int} = 0.0534, R_{sigma} = 0.0280) which were used in all calculations. The final R_1 was 0.0584 (I >2σ(I)) and wR_2 was 0.1318 (all data).

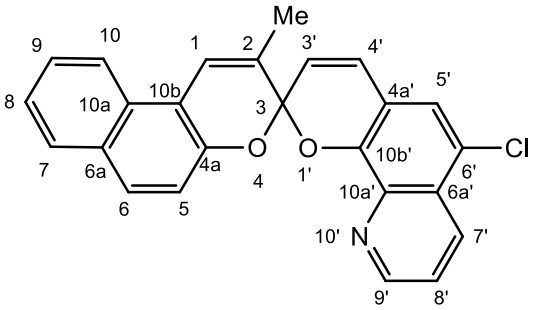

*B. Synthesis of spirobipyran **1***

6'-Chloro-2-methylspiro[benzo[*f*]chromene-3,2'-pyrano[3,2-*h*]quinoline] (1). Aldehyde **2** (0.21 g, 1 mmol) was added to a boiling solution of benzochromenium perchlorate **3** (0.31 g, 1 mmol) in acetic acid (12 ml). The mixture was refluxed for 2 h and kept at ~ 20 °C for 12 h. The formed precipitate was filtered off, washed with ether, dried, and used without further purification. A stream of dry ammonia was passed into a suspension of the obtained salt in chloroform (15 ml) until the precipitate was dissolved. The solvent was evaporated, the residual precipitate was purified by column chromatography on Al_2O_3 (eluent chloroform) and recrystallized. The yield is 40%. M. p. 192-194°C (toluene). ^{1}H NMR (300 MHz, $CDCl_3$, δ ppm): 8.80 (dd, J = 4.2, 1.7, 1H, H-9'), 8.45 (dd, J = 8.6, 1.7, 1H, H-7'), 8.12 (d, J = 8.4, 1H, H-10), 7.73 (ddd, J = 8.1, 1.2, 0.6, 1H, H-7), 7.58 (d, J = 8.9, 1H, H-6), 7.52 (ddd, J = 8.4, 6.8, 1.4, 1H, H-9), 7.51 (s, 1H, H-5'), 7.41-7.42 (m, 1H, H-1), 7.39 (dd, J = 8.6, 4.2, 1H, H-8'), 7.36 (ddd, J = 8.1, 6.9, 1.1, 1H, H-8), 6.97 (d, J = 9.6, 1H, H-4'), 6.94 (d, J = 8.9, 1H, H-5), 6.20 (d, J = 9.6, 1H, H-3'), 2.17 (d, J = 1.5, 3H, C-CH_3). ^{13}C NMR (75 MHz, $CDCl_3$) δ: 150.53 (C-9'), 147.30 (C-4a), 145.38 (C-10b'), 140.20 (C-10a'), 132.76 (C-7'), 129.65 (C-6a), 129.41 (C-10a), 129.11 (C-6), 128.50 (C-7), 127.14 (C-6a'), 127.08 (C-2), 126.59 (C-9), 125.77 (C-5), 124.92 (C-5'), 123.90 (C-8), 123.09 (C-6'), 122.15 (C-3'), 122.01 (C-8'), 121.47 (C-10), 119.93 (C-1), 117.89 (C-4a'), 117.55(C-4'), 113.12 (C-10b), 99.32 (2'/3-C), 20.25 (CH_3). Elemental analyses:

Found: C, 75.44; H, 4.09; N, 8.96%; $C_{25}H_{16}ClNO_2$; requires: C, 75.47; H, 4.05; N, 3.52 %. MS (ESI-TOF) m/z: found: 398.0947 $[M+H]^+$ $C_{25}H_{16}ClNO_2$. Calc: 398.0942.

C. Experimental data

NMR spectra

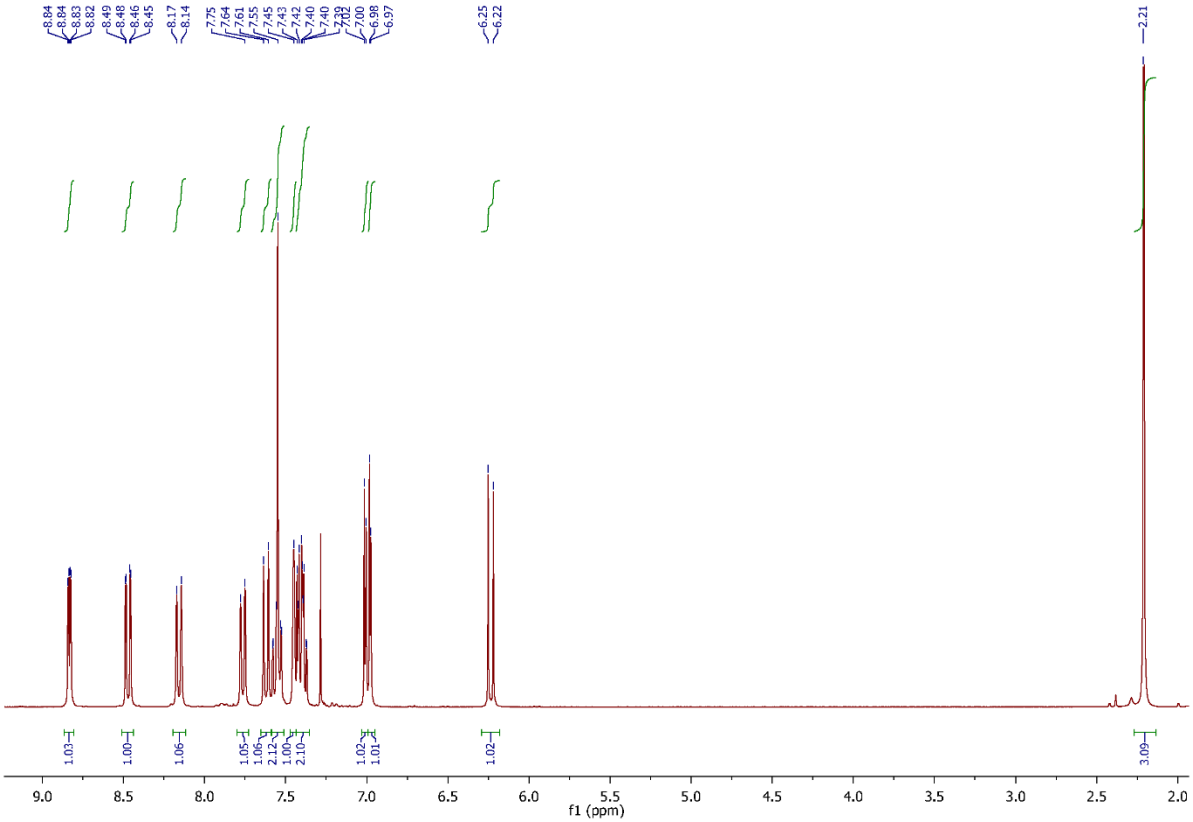

Figure S1. NMR^{1}H spectrum of compound **1**

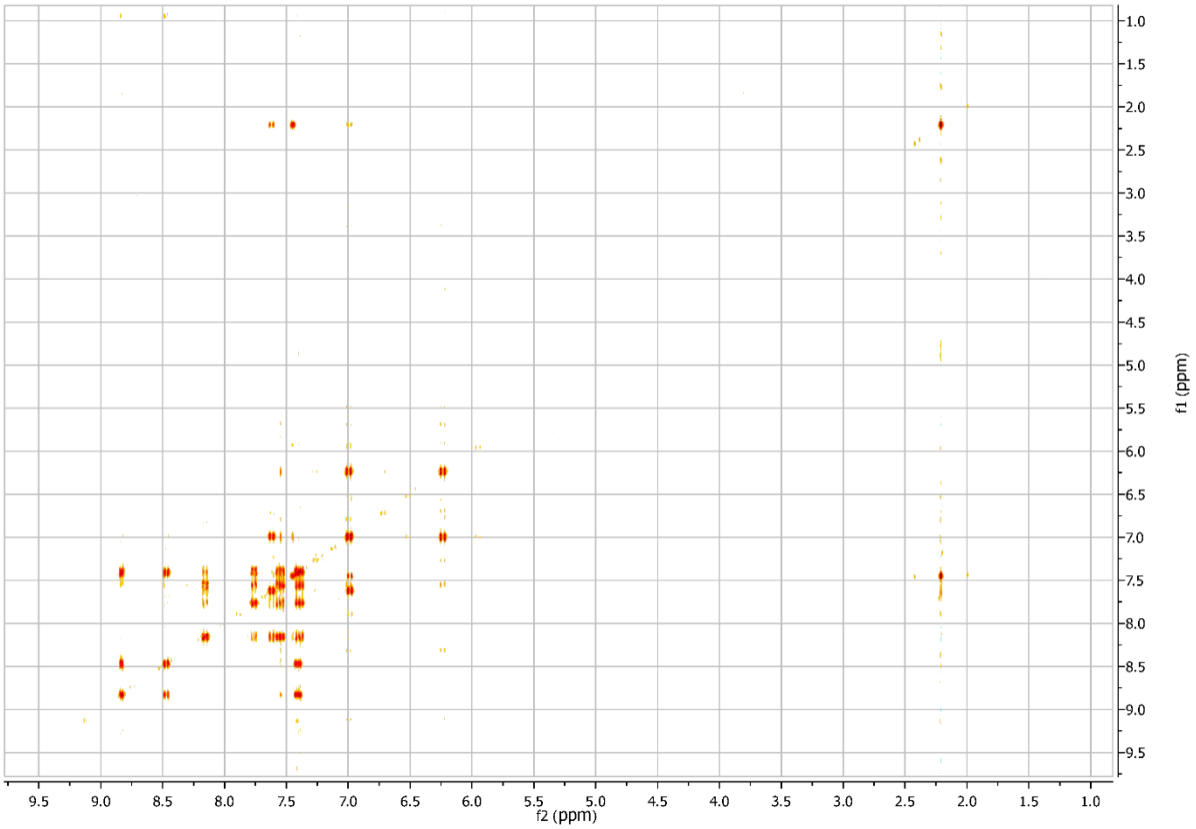

Figure S2. COSY ^{1}H-^{1}HNMR spectrum of**1**

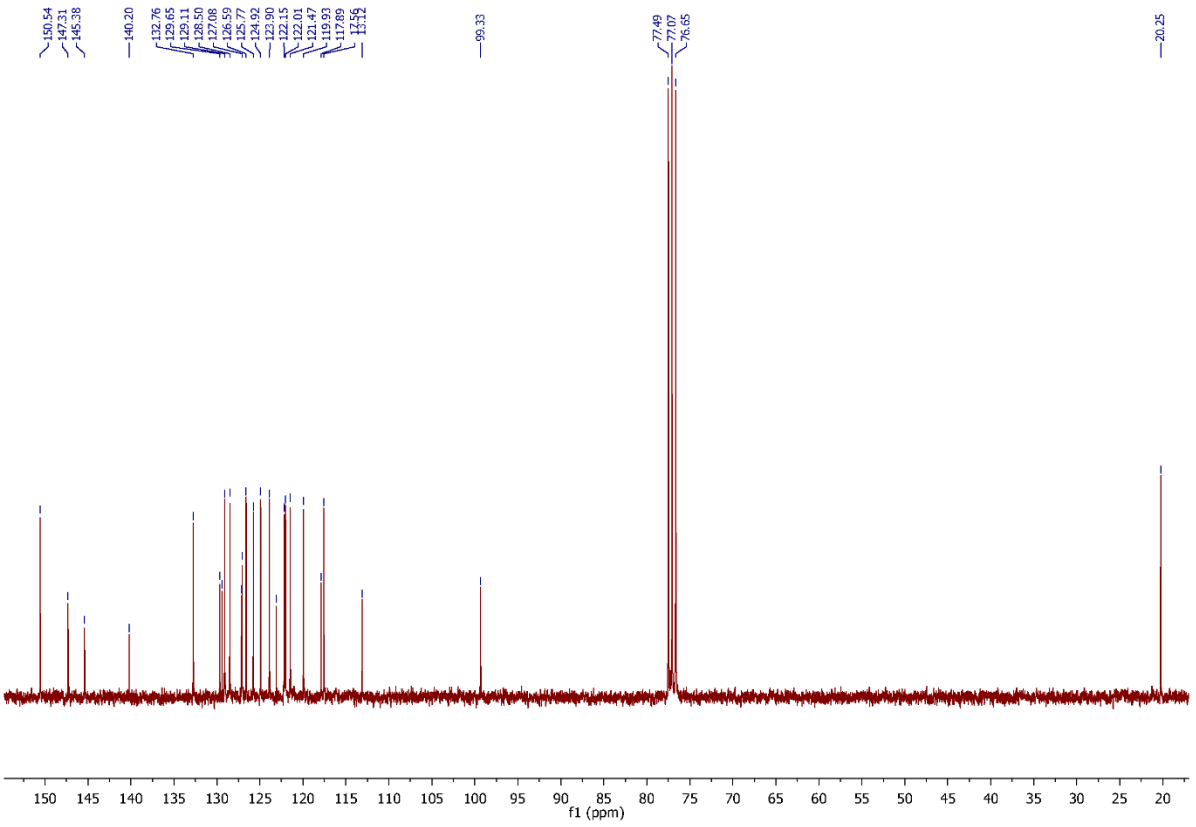

Figure S3. NMR^{13}C spectrum of **1**

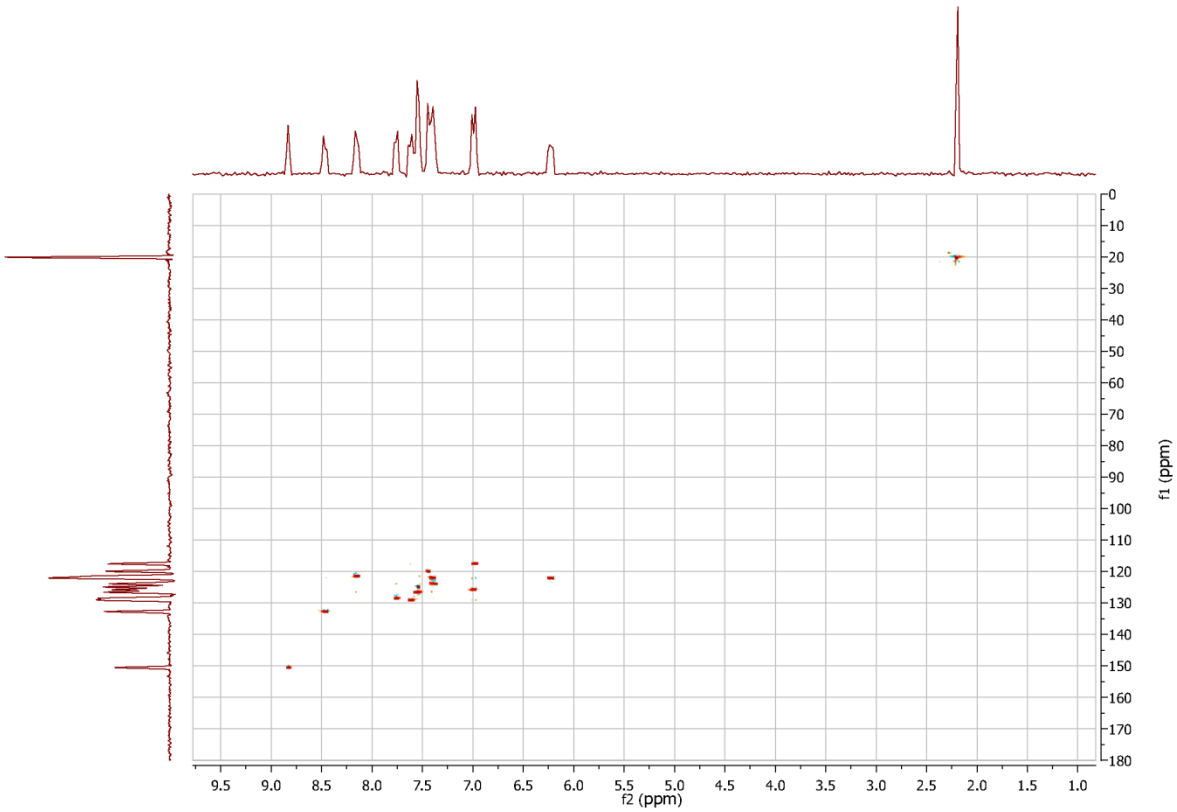

Figure S4. HSQC ^{1}H-^{13}C NMR spectrum of **1**

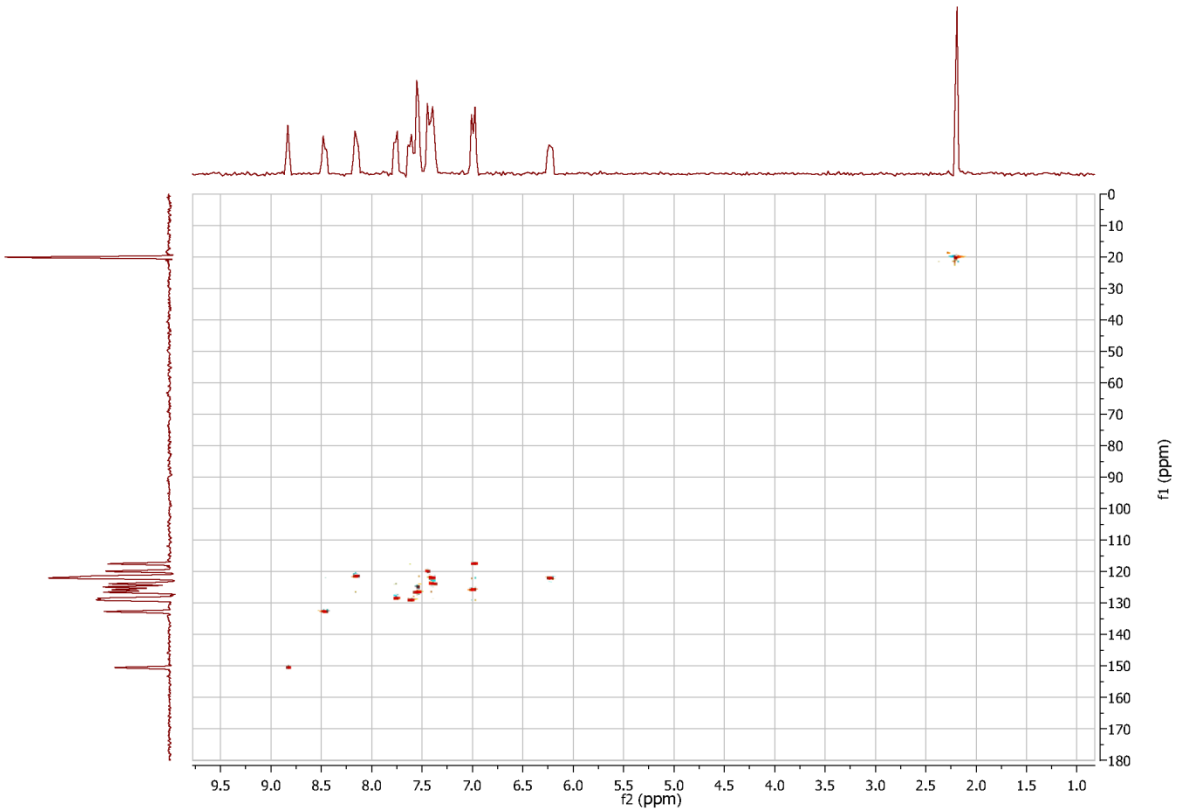

Figure S5. HMBC ^{1}H-^{13}C NMR spectrum of **1**

Mass spectrum

Figure S6. ESI-MS spectrum of **1**

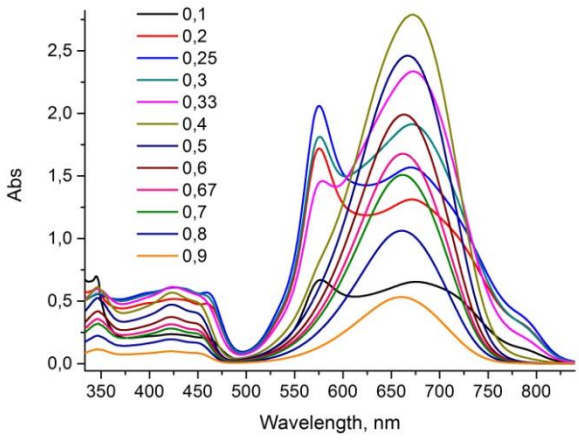

Figure S7. Absorption spectra of the isomolar series of solution **1** with zinc (C(Zn)+C(**1**) = $8.0 \cdot 10^{-5}$ M), the numbers on a graph indicate the zinc molar fraction.

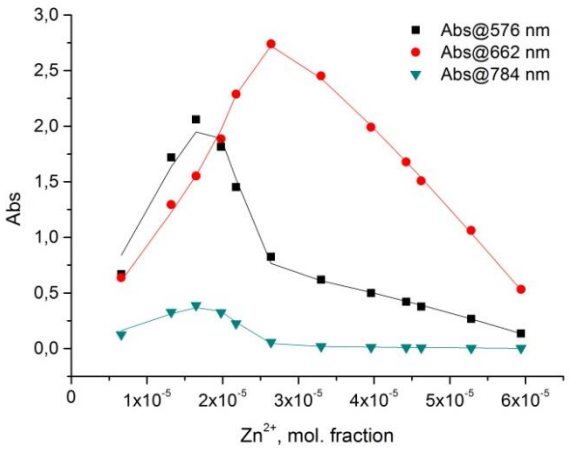

Figure S8. Continuous variation plot of **1** with zinc at the characteristic observation wavelengths. Points are experimental data, curves are calculated values.

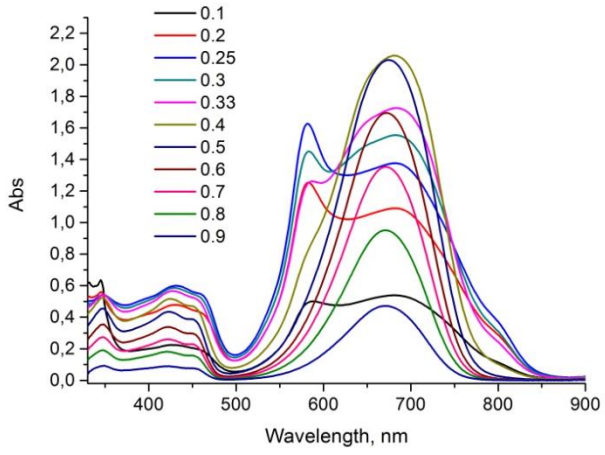

Figure S9. Absorption spectra of the isomolar series of solution **1** with cobalt (C(Co)+C(**1**) = $7.0 \cdot 10^{-5}$ M), the numbers on a graph indicate the cobalt molar fraction.

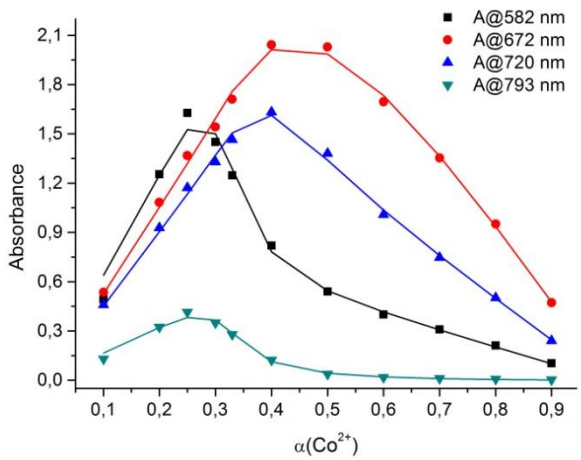

Figure S10. Continuous variation plot of **1** with cobalt at the characteristic observation wavelengths. Points are experimental data, curves are calculated values.

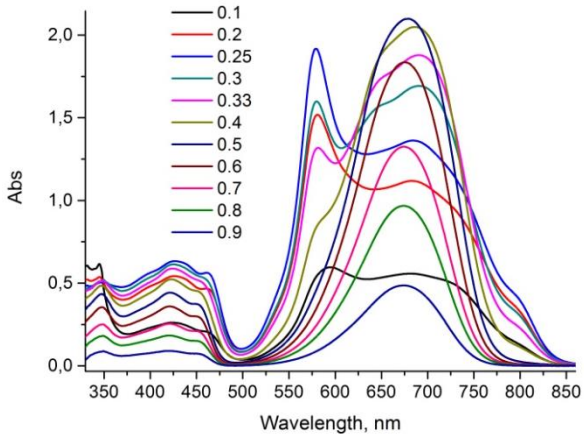

Figure S11. Absorption spectra of the isomolar series of solution **1** with nickel (C(Ni)+C(**1**) = $7.0 \cdot 10^{-5}$ M), the numbers on a graph indicate the cobalt molar fraction.

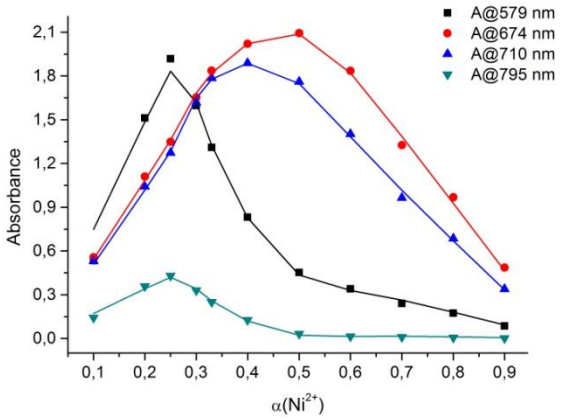

Figure S12. Continuous variation plot of **1** with nickel at the characteristic observation wavelengths. Points are experimental data, curves are calculated values.

Complex formation of SBP with metal ions in solution can be presented as a set of coupled equilibriums:

$$A \rightleftharpoons B$$

$$B + M \rightleftharpoons MB$$

$$B + MB \rightleftharpoons MB_2$$

$$B + MB_2 \rightleftharpoons MB_3$$

These equilibriums are described by the following constants:

$$K_T = \frac{[B]}{[A]} \quad (1)$$

$$K_1 = \frac{[MB]}{[B][M]} \quad (2)$$

$$K_2 = \frac{[MB_2]}{[MB][B]} \quad (3)$$

$$K_3 = \frac{[MB_3]}{[MB_2][B]} \quad (4)$$

The SBP merocyanine isomer concentration in acetone is very low to estimate equilibrium quantitatively using NMR technique and thus the subsequent calculation of K_T is impossible. Therefore, we have calculated effective stability constants taking into account tautomeric equilibrium of the ligand:

$$K_i^{\text{eff}} = \frac{[MB_i]}{[MB_{i-1}][L]^i}, \quad (5)$$

where $[L] = [B] + [A] = C_{SBP} - \sum_i i[MB_i]$ equilibrium concentration of uncomplexated SPP forms, C_{SPP} and C_M are the total concentration of the spiropyran and metal ion, respectively. K_i^{eff} values

are essential for practical calculations of complexation degree and prediction of metal ion binding extent in real conditions, this being important for application of such compounds in analytical chemistry.

Stability constants K_i^{eff} have been determined based on the absorbance dependences of solutions containing isomolar quantity of SPP and metal perchlorate. The calculation is based on the minimization of the functional (5) by varying K_i and ε_{MBi} values which are subjects of determination:

$$F = \sum_{i=1}^{n_s} \sum_{j=1}^{n_\lambda} \left(A_{obs} - A_{calc}\right)^2 \rightarrow \min \ , \qquad (5)$$

where n_S - number of solutions, $n\lambda$ - number of observation wavelengths.

$$A_{calc} = \varepsilon_{MB}[MB] + \varepsilon_{MB_2}[MB_2] + \varepsilon_{MB_3}[MB_3] + \varepsilon_L^{eff}[L] + \varepsilon_M[M]$$

$$[MB] = \frac{C_M K_1^{eff}[L]}{1 + K_1^{eff}[L] + K_1^{eff} K_2^{eff}[L]^2 + K_1^{eff} K_2^{eff} K_3^{eff}[L]^3}$$

$$[MB_2] = \frac{C_M K_1^{eff} K_2^{eff}[L]^2}{1 + K_1^{eff}[L] + K_1^{eff} K_2^{eff}[L]^2 + K_1^{eff} K_2^{eff} K_3^{eff}[L]^3}$$

$$[MB_3] = \frac{C_M K_1^{eff} K_2^{eff} K_3^{eff}[L]^3}{1 + K_1^{eff}[L] + K_1^{eff} K_2^{eff}[L]^2 + K_1^{eff} K_2^{eff} K_3^{eff}[L]^3}$$

$$C_{SBP} = [MB] + 2[MB_2] + 3[MB_3] + [L]$$

$$C_M = [MB] + [MB_2] + [MB_3] + [M]$$

Parameters A_{obs} and A_{calc} are observed and calculated values of absorbance at the selected wavelength, respectively. For minimization of the functional (5) the Newton-Gauss algorithm has been employed [S5]. In an iterative nonlinear procedure, the dependences of absorbance *vs.* concentration of metal salt at 200 selected wavelengths have been used. In Figures S7, S9, S11 absorption spectra of SBP **1** in the presence of metal ions are presented. As it is seen from the picture, the position and intensity of the long-wavelength absorption band significantly depend on the ratio of initial concentrations of SBP **1** and the metal ion. Theoretically calculated absorbance *vs* metal mole fraction for given total concentration dependences at the characteristic wavelengths are in a good agreement with experimental data.

Table S1 Crystal data and structure refinement for 1.

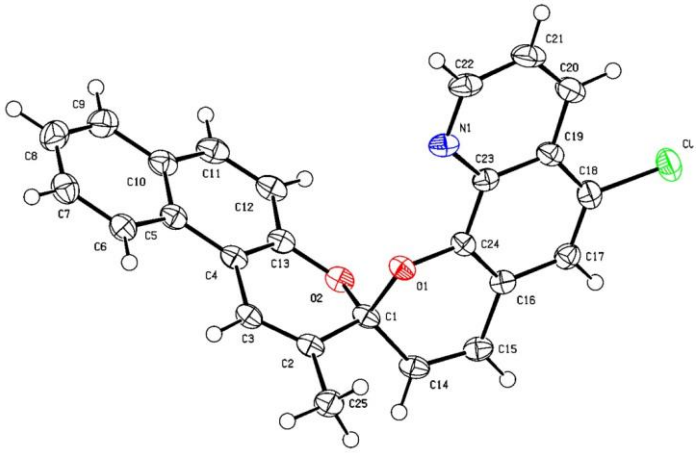

CCDC Number	2123459
Empiricalformula	$C_{25}H_{16}ClNO_2$
Formulaweight	397.84
Temperature/K	100.00(10)
Crystalsystem	orthorhombic
Spacegroup	Pbca
a/Å	11.5038(3)
b/Å	6.5637(2)
c/Å	49.8431(14)
α/°	90
β/°	90
γ/°	90
Volume/Å^3	3763.53(18)
Z	8
ρ_{calc}g/cm^3	1.404
μ/mm^{-1}	1.972
F(000)	1648.0
Crystalsize/mm^3	0.629 × 0.328 × 0.308
Radiation	Cu Kα (λ = 1.54184)
2Θ range for data collection/°	7.094 to 154.032
Indexranges	$-13 \leq h \leq 14$, $-8 \leq k \leq 7$, $-62 \leq l \leq 53$
Reflectionscollected	20085
Independentreflections	3945 [R_{int} = 0.0534, R_{sigma} = 0.0280]
Data/restraints/parameters	3945/0/263
Goodness-of-fit on F^2	1.104
Final R indexes [I>=2σ (I)]	R_1 = 0.0584, wR_2 = 0.1257
Final R indexes [all data]	R_1 = 0.0641, wR_2 = 0.1318
Largest diff. peak/hole / e Å^{-3}	0.26/-0.40

Table S2 Fractional atomic coordinates ($\times 10^4$) and equivalent isotropic displacement parameters ($Å^2 \times 10^3$) for 637_file004. U_{eq} is defined as 1/3 of the trace of the orthogonalised U_{IJ} tensor.

Atom	*x*	*y*	*z*	U(eq)
Cl	3423.7(6)	5828.3(11)	5045.0(2)	37.05(18)
O1	5546.3(13)	3819(2)	6088.2(3)	23.0(3)
O2	3979.2(13)	3843(3)	6381.4(3)	25.2(4)
N1	6238.7(17)	7234(3)	5836.9(4)	26.4(4)
C16	4184.8(19)	3037(4)	5739.5(5)	23.1(5)
C24	5018.6(19)	4294(4)	5850.2(4)	21.8(4)
C4	5187.9(19)	4887(4)	6749.2(4)	23.0(5)
C13	4254.7(19)	5213(4)	6580.9(5)	24.2(5)
C19	4901(2)	6581(4)	5463.2(5)	25.4(5)
C3	5866(2)	3049(4)	6705.6(5)	24.5(5)
C14	4249(2)	909(4)	6132.2(5)	26.9(5)
C5	5399(2)	6343(4)	6956.9(5)	25.6(5)
C1	4888.6(19)	2581(4)	6273.6(4)	23.5(5)
C17	3701(2)	3548(4)	5486.1(5)	26.3(5)
C23	5401.0(19)	6074(3)	5716.1(5)	22.9(5)
C15	3877(2)	1189(4)	5882.1(5)	27.0(5)
C18	4047(2)	5259(4)	5355.5(5)	28.0(5)
C2	5745(2)	1913(4)	6485.4(5)	24.2(5)
C6	6360(2)	6195(4)	7134.5(5)	28.3(5)
C10	4633(2)	8022(4)	6988.7(5)	29.4(5)
C12	3488(2)	6867(4)	6609.6(5)	28.8(5)
C11	3681(2)	8229(4)	6812.0(5)	31.9(5)
C20	5318(2)	8367(4)	5336.4(5)	34.1(6)
C22	6586(2)	8891(4)	5709.5(5)	32.7(6)
C7	6526(2)	7596(4)	7334.0(5)	33.3(6)
C25	6477(2)	87(4)	6426.8(5)	32.9(6)
C9	4834(2)	9450(4)	7195.8(5)	35.3(6)
C21	6150(3)	9510(4)	5458.4(6)	37.2(6)
C8	5755(3)	9246(4)	7366.8(5)	37.4(6)

Table S3 Bond lengths for compound **1.**

Atom	Atom	Length/Å	Atom	Atom	Length/Å
Cl	C18	1.746(2)	C19	C20	1.415(3)
O1	C24	1.368(3)	C3	C2	1.334(3)
O1	C1	1.445(3)	C14	C1	1.498(3)
O2	C13	1.378(3)	C14	C15	1.331(3)
O2	C1	1.438(3)	C5	C6	1.419(3)
N1	C23	1.368(3)	C5	C10	1.420(3)
N1	C22	1.321(3)	C1	C2	1.509(3)
C16	C24	1.380(3)	C17	C18	1.358(4)
C16	C17	1.421(3)	C2	C25	1.494(3)
C16	C15	1.450(3)	C6	C7	1.368(4)
C24	C23	1.416(3)	C10	C11	1.412(4)
C4	C13	1.379(3)	C10	C9	1.413(4)
C4	C3	1.453(3)	C12	C11	1.366(4)
C4	C5	1.430(3)	C20	C21	1.359(4)
C13	C12	1.406(3)	C22	C21	1.409(4)
C19	C23	1.425(3)	C7	C8	1.410(4)
C19	C18	1.416(4)	C9	C8	1.366(4)

Table S4 Bond angles for compound **1.**

Atom	Atom	Atom	Angle/°	Atom	Atom	Atom	Angle/°
C24	O1	C1	116.76(17)	O2	C1	C14	103.91(18)
C13	O2	C1	118.56(17)	O2	C1	C2	112.40(19)
C22	N1	C23	117.4(2)	C14	C1	C2	115.9(2)
C24	C16	C17	119.1(2)	C18	C17	C16	120.4(2)
C24	C16	C15	118.3(2)	N1	C23	C24	118.1(2)
C17	C16	C15	122.5(2)	N1	C23	C19	122.9(2)
O1	C24	C16	121.3(2)	C24	C23	C19	119.0(2)
O1	C24	C23	117.3(2)	C14	C15	C16	119.7(2)
C16	C24	C23	121.3(2)	C19	C18	Cl	119.32(19)
C13	C4	C3	117.1(2)	C17	C18	Cl	118.8(2)
C13	C4	C5	118.0(2)	C17	C18	C19	121.9(2)
C5	C4	C3	124.9(2)	C3	C2	C1	118.8(2)
O2	C13	C4	121.1(2)	C3	C2	C25	123.4(2)
O2	C13	C12	115.7(2)	C25	C2	C1	117.7(2)
C4	C13	C12	123.1(2)	C7	C6	C5	121.1(2)
C18	C19	C23	118.2(2)	C11	C10	C5	119.1(2)
C20	C19	C23	116.8(2)	C11	C10	C9	121.2(2)
C20	C19	C18	125.0(2)	C9	C10	C5	119.7(2)
C2	C3	C4	122.1(2)	C11	C12	C13	118.6(2)
C15	C14	C1	119.8(2)	C12	C11	C10	121.6(2)
C6	C5	C4	122.6(2)	C21	C20	C19	119.7(2)
C6	C5	C10	117.8(2)	N1	C22	C21	123.8(3)
C10	C5	C4	119.6(2)	C6	C7	C8	120.8(3)
O1	C1	C14	111.64(19)	C8	C9	C10	121.2(3)
O1	C1	C2	105.60(17)	C20	C21	C22	119.3(2)
O2	C1	O1	107.19(18)	C9	C8	C7	119.4(3)

Table S5 Torsion angles for compound **1.**

A	B	C	D	Angle/°	A	B	C	D	Angle/°
O1	C24	C23	N1	-2.2(3)	C5	C4	C3	C2	-169.4(2)
O1	C24	C23	C19	177.82(19)	C5	C6	C7	C8	-0.8(4)
O1	C1	C2	C3	91.9(2)	C5	C10	C11	C12	-0.8(4)
O1	C1	C2	C25	-83.7(3)	C5	C10	C9	C8	0.0(4)
O2	C13	C12	C11	177.0(2)	C1	O1	C24	C16	-27.3(3)
O2	C1	C2	C3	-24.6(3)	C1	O1	C24	C23	155.54(19)
O2	C1	C2	C25	159.7(2)	C1	O2	C13	C4	-26.1(3)
N1	C22	C21	C20	0.3(4)	C1	O2	C13	C12	157.6(2)
C16	C24	C23	N1	-179.3(2)	C1	C14	C15	C16	5.7(4)
C16	C24	C23	C19	0.7(3)	C17	C16	C24	O1	-177.2(2)
C16	C17	C18	Cl	-179.80(18)	C17	C16	C24	C23	-0.2(3)
C16	C17	C18	C19	0.6(4)	C17	C16	C15	C14	-171.9(2)
C24	O1	C1	O2	-72.0(2)	C23	N1	C22	C21	-0.4(4)
C24	O1	C1	C14	41.1(3)	C23	C19	C18	Cl	-179.63(17)
C24	O1	C1	C2	167.93(19)	C23	C19	C18	C17	0.0(3)

A	B	C	D	Angle/°	A	B	C	D	Angle/°
C24	C16	C17	C18	-0.5(3)	C23	C19	C20	C21	-0.5(3)
C24	C16	C15	C14	10.9(3)	C15	C16	C24	O1	0.1(3)
C4	C13	C12	C11	0.7(4)	C15	C16	C24	C23	177.1(2)
C4	C3	C2	C1	0.9(3)	C15	C16	C17	C18	-177.6(2)
C4	C3	C2	C25	176.2(2)	C15	C14	C1	O1	-30.9(3)
C4	C5	C6	C7	-178.9(2)	C15	C14	C1	O2	84.3(3)
C4	C5	C10	C11	-0.6(3)	C15	C14	C1	C2	-151.9(2)
C4	C5	C10	C9	179.3(2)	C18	C19	C23	N1	179.4(2)
C13	O2	C1	O1	-78.5(2)	C18	C19	C23	C24	-0.6(3)
C13	O2	C1	C14	163.19(18)	C18	C19	C20	C21	-179.4(2)
C13	O2	C1	C2	37.1(3)	C6	C5	C10	C11	178.9(2)
C13	C4	C3	C2	12.3(3)	C6	C5	C10	C9	-1.1(3)
C13	C4	C5	C6	-177.6(2)	C6	C7	C8	C9	-0.4(4)
C13	C4	C5	C10	1.9(3)	C10	C5	C6	C7	1.6(3)
C13	C12	C11	C10	0.8(4)	C10	C9	C8	C7	0.9(4)
C19	C20	C21	C22	0.2(4)	C11	C10	C9	C8	179.9(2)
C3	C4	C13	O2	0.3(3)	C20	C19	C23	N1	0.4(3)
C3	C4	C13	C12	176.4(2)	C20	C19	C23	C24	-179.6(2)
C3	C4	C5	C6	4.2(4)	C20	C19	C18	Cl	-0.7(3)
C3	C4	C5	C10	-176.3(2)	C20	C19	C18	C17	178.9(2)
C14	C1	C2	C3	-143.9(2)	C22	N1	C23	C24	-180.0(2)
C14	C1	C2	C25	40.5(3)	C22	N1	C23	C19	0.0(3)
C5	C4	C13	O2	-178.09(19)	C9	C10	C11	C12	179.3(2)
C5	C4	C13	C12	-2.0(3)					

Table S6 Hydrogen atom coordinates ($Å \times 10^4$) and isotropic displacement parameters ($Å^2 \times 10^3$) for compound **1.**

Atom	*x*	*y*	*z*	U(eq)
H3	6411.81	2642.32	6838.2	29
H14	4109.16	-349.1	6220.88	32
H17	3130.79	2687.47	5407.44	32
H15	3410.53	182.02	5797.37	32
H6	6895.81	5104.23	7114.57	34
H12	2849.18	7034.53	6490.86	35
H11	3162.84	9342.3	6834.41	38
H20	5017.35	8765.36	5166.82	41
H22	7163.88	9713	5792.12	39
H7	7170.13	7456.28	7451.91	40
H25A	7014.86	400.14	6279.98	49
H25B	5976.07	-1053.8	6374.57	49
H25C	6920.72	-284.32	6587.38	49
H9	4320.46	10572.14	7216.32	42
H21	6433.33	10712.99	5375.09	45
H8	5873.53	10207.19	7506.6	45

References

S1. *CrysAlisPro*, *version 171.41.93a*, Rigaku Oxford Diffraction, 2015. https://www.rigaku.com/products/crystallography/crysalis.

S2. G. M. Sheldrick, *Acta Crystallogr*., *Sect. A: Found. Adv.*, 2015, **71**, 3.

S3. G. M. Sheldrick, *Acta Crystallogr*., *Sect. C: Struct. Chem.*, 2015, **71**, 3.

S4. O. V Dolomanov, L. J. Bourhis, R. J. Gildea, J. A. K. Howard, H. Puschmann, *J. Appl. Crystallogr.*, 2009, **42**, 339.

S5. S. A. Merny, D. S. Konyaev, Yu. V. Kholin, *Kharkov Univ. Bull.*, 1998, **420**, 112.